Indian Heart Journal 72 (2020) 258–264

Contents lists available at ScienceDirect

Indian Heart Journal

journal homepage: www.elsevier.com/locate/ihj

Original Article

Cardiovascular/stroke risk prevention: A new machine learning framework integrating carotid ultrasound image-based phenotypes and its harmonics with conventional risk factors

Ankush Jamthikar [a], Deep Gupta [a], Narendra N. Khanna [b], Luca Saba [c], John R. Laird [d], Jasjit S. Suri [e, *]

[a] Department of Electronics and Communication Engineering, Visvesvaraya National Institute of Technology, Nagpur, Maharashtra, India
[b] Department of Cardiology, Indraprastha APOLLO Hospitals, New Delhi, India
[c] Department of Radiology, University of Cagliari, Italy
[d] Heart and Vascular Institute, Adventist Health St. Helena, St Helena, CA, USA
[e] Stroke Monitoring and Diagnostic Division, AtheroPoint™, Roseville, CA, USA

ARTICLE INFO

Article history:
Received 9 May 2019
Accepted 10 June 2020
Available online 18 June 2020

Keywords:
Atherosclerosis
Conventional risk factors
Covariates
Carotid
Ultrasound
Image-based phenotypes
10-Year measurements
Harmonics
Features
AtheroRisk-integrated
AtheroRisk-conventional

ABSTRACT

Motivation: Machine learning (ML)-based stroke risk stratification systems have typically focused on conventional risk factors (CRF) (*AtheroRisk-conventional*). Besides CRF, carotid ultrasound image phenotypes (CUSIP) have shown to be powerful phenotypes risk stratification. This is the first ML study of its kind that integrates CUSIP and CRF for risk stratification (*AtheroRisk-integrated*) and compares against *AtheroRisk-conventional*.

Methods: Two types of ML-based setups called (i) *AtheroRisk-integrated* and (ii) *AtheroRisk-conventional* were developed using random forest (RF) classifiers. *AtheroRisk-conventional* uses a feature set of 13 CRF such as age, gender, hemoglobin A1c, fasting blood sugar, low-density lipoprotein, and high-density lipoprotein (HDL) cholesterol, total cholesterol (TC), a ratio of TC and HDL, hypertension, smoking, family history, triglyceride, and ultrasound-based carotid plaque score. *AtheroRisk-integrated* system uses the feature set of 38 features with a combination of 13 CRF and 25 CUSIP features (6 types of current CUSIP, 6 types of 10-year CUSIP, 12 types of quadratic CUSIP (harmonics), and age-adjusted grayscale median). Logistic regression approach was used to select the significant features on which the RF classifier was trained. The performance of both ML systems was evaluated by area-under-the-curve (AUC) statistics computed using a leave-one-out cross-validation protocol.

Results: Left and right common carotid arteries of 202 Japanese patients were retrospectively examined to obtain 404 ultrasound scans. RF classifier showed higher improvement in AUC (**~57%**) for leave-one-out cross-validation protocol. Using RF classifier, AUC statistics for *AtheroRisk-integrated* system was higher (AUC = **0.99**,p-value<0.001) compared to *AtheroRisk-conventional* (AUC = **0.63**,p-value<0.001).

Conclusion: The *AtheroRisk-integrated* ML system outperforms the *AtheroRisk-conventional* ML system using RF classifier.

1. Introduction

Cardiovascular disease (CVD) and stroke are the major global challenges for public healthcare.[1] The CVD/stroke risk assessment using statistically-derived risk prediction models can support in the prevention and management of these diseases.[2–8] But such statistically-derived models either underestimate or overestimate risk CVD risk in certain patients.[9–15] The primary reason for this poor performance is the dependence of such models on the cardiovascular risk factors (CRF) that does not provide complete information about cardiovascular health of patients.[16–20]

Non-invasive ultrasound imaging of carotid arteries can capture the morphological variations in atherosclerotic plaque components.[16–25] These variations are indicated using the carotid intima-media thickness (cIMT) and carotid plaque (CP) (Fig. 1),

* Corresponding author. AtheroPoint™, Roseville, CA, 95661, USA. Fax: +916 797 4942.
E-mail address: jasjit.suri@atheropoint.com (J.S. Suri).

https://doi.org/10.1016/j.ihj.2020.06.004

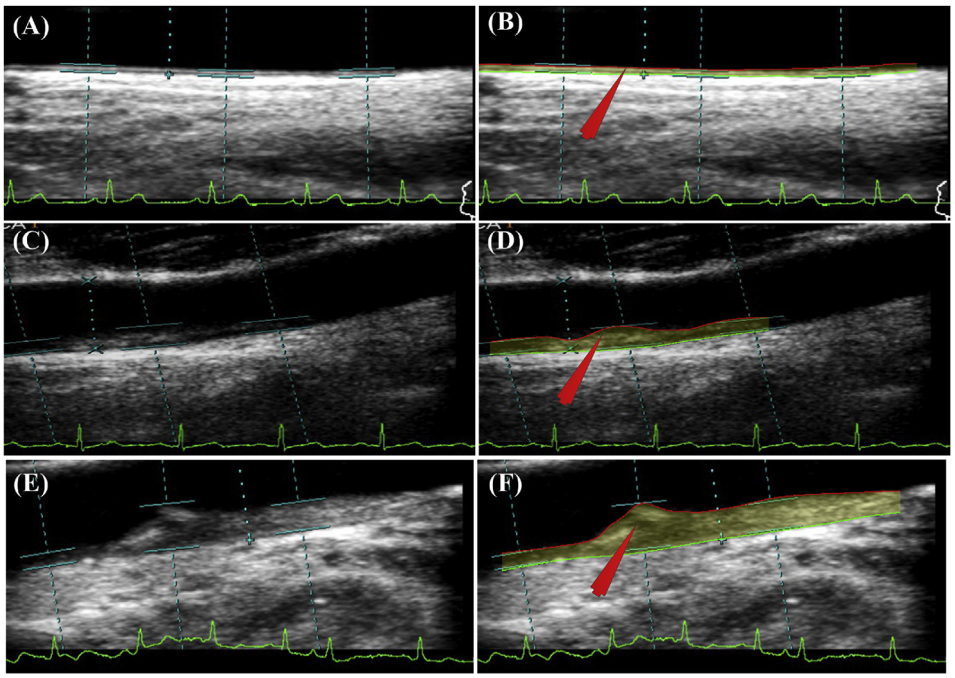

Fig. 1. Risk stratification based on automated $CUSIP_{curr}$ and $CUSIP_{10yr}$. **Row 1 - Patient 70L (low-risk)**: (A) Original Image; (B) Processed image using AtheroEdge™ 2.0; $CUSIP_{curr}$: $cIMT_{ave}$ = 0.47 mm, $cIMT_{max}$ = 0.6 mm, $cIMT_{min}$ = 0.35 mm, cIMTV = 0.07 mm, and TPA = 14.96 mm^2, $AECRS_{curr}$ = 7.81%; $CUSIP_{10yr}$:$cIMT_{ave10yr}$ = 0.56 mm, $cIMT_{max10yr}$ = 0.71 mm, $cIMT_{min10yr}$ = 0.36 mm, $cIMTV_{10yr}$ = 0.07 mm, and TPA_{10yr} = 17.87 mm^2, $AECRS_{10yr}$ = 10.15%. **Row 2 - Patient 103R (moderate-risk):** (C) Original Image; (D) Processed image using AtheroEdge™ 2.0; $CUSIP_{curr}$: $cIMT_{ave}$ = 0.82 mm, $cIMT_{max}$ = 1.01 mm, $cIMT_{min}$ = 0.53 mm, cIMTV = 0.14 mm, and TPA = 27.32 mm^2, $AECRS_{curr}$ = 25.94%; $CUSIP_{10yr}$: $cIMT_{ave10yr}$ = 0.84 mm, $cIMT_{max10yr}$ = 1.02 mm, $cIMT_{min10yr}$ = 0.69 mm, $cIMTV_{10yr}$ = 0.15 mm, and TPA_{10yr} = 28.07 mm^2, $AECRS_{10yr}$ = 46.65%. **Row 3 - Patient 110L (high-risk):** (E) Original Image; (F) Processed image using AtheroEdge™ 2.0; $CUSIP_{curr}$: $cIMT_{ave}$ = 2.18 mm, $cIMT_{max}$ = 3.53 mm, $cIMT_{min}$ = 0.77 mm, cIMTV = 0.87 mm, and TPA = 71 mm^2, $AECRS_{curr}$ = 75.28%; $CUSIP_{curr}$: $cIMT_{ave10yr}$ = 2.26 mm, $cIMT_{max10yr}$ = 3.76 mm, $cIMT_{min10yr}$ = 0.78 mm, $cIMTV_{10yr}$ = 0.88 mm, and TPA_{10yr} = 73.06 mm^2, $AECRS_{10yr}$ = 80.30%. (AECRS: AtheroEdge Composite Risk Score, TPA: Total Plaque Area, $cIMT_{ave}$: Average cIMT, $cIMT_{max}$: Maximum cIMT, $cIMT_{min}$: Minimum cIMT, cIMTV: Variations in cIMT; 'curr' indicates present value and '10-yr' indicates value after 10 years).

which are also considered as the surrogate markers of coronary heart disease (CHD).[26,27] In recent years multiple automated carotid ultrasound image-based phenotypes (CUSIP) were derived,[21,28–32] which can provide better CVD/stroke risk stratification, when combined with the conventional risk factors. In order to ease the image analysis and further improve the accuracy of the risk stratification artificial intelligence techniques such as machine learning (ML) algorithms are widely adopted.[33–36] The ML algorithms are data-driven techniques that classify the patients into risk categories based on various complex interactions between input risk predictors.[16,37–39] ML algorithms minimize the intra- and inter-operator variability CUSIP measurements, and, therefore, perform better compared to conventional statistically-derived risk calculators.[37,40]

The objective of this study is to predict the risk of CVD/stroke using an ML framework on retrospective data while using the event-equivalence gold standard (EEGS) as the surrogate endpoints. Since our dataset is retrospective and does not have primary endpoints (like cerebrovascular or cardiovascular events), we, therefore, use event-equivalence gold standards (EEGS). The carotid lumen diameter (LD) has been used as an EEGS in our study. The justification of EEGS is exclusively discussed in the next section. This study introduces an ML-based framework that integrates CUSIP with CRF for risk stratification (so-called *AtheroRisk-integrated* system, a class of AtheroEdge™ systems, CA, USA). This is similar to CVD risk being estimated by integrating (a) wall phenotypes (such as wall thickness, lumen area, vessel area, or atheroma area) with (b) grayscale wall-based texture features for better performance[41]. Since imaging of the carotid artery phenotypes may offer insight into CVD/stroke risk not evident from conventional features alone, we hypothesize that the *AtheroRisk-integrated* system would show a greater area-under-the-curve (AUC) in predicting the CVD/stroke compared to *AtheroRisk-conventional* system. The acronyms used in this study are tabulated in Table A and Table B under Section A of the Supplementary Material.

2. Event-equivalence gold standard

Cardiovascular and/or cerebrovascular mortalities are often considered as the primary endpoint to evaluate any clinical studies.[42, 43] However, such primary endpoints are expensive and time-consuming.[44] Furthermore, they require a large number of samples with long follow-up duration.[42, 43] Thus, there is a need to search for secondary endpoints or surrogate biomarkers that can mimic the behavior of the primary endpoints.[27, 42, 43, 45] Such endpoints can be used as a gold standard for assessing the risk of future CV events with fewer sample sizes, at a lower cost, and with shorter study duration.[42, 43] Since these gold standards are the alternatives to the primary endpoints, we can thus call them as the event-equivalence gold standards (EEGS).

Note that atherosclerosis is developed by the accumulation of calcium, lipid, collagen, fibrosis, macrophages, and other similar substances within the walls of the blood vessels.[27] Furthermore, the progression of atherosclerosis is highly associated with the future risk of CV or stroke events.[46, 47] Thus, the EEGS is the one that explains the progression of atherosclerosis disease.[42, 43] Carotid lumen diameter (LD) reflects the growth in atherosclerosis and also considered as a risk factor of cardiovascular diseases.[48] Furthermore, carotid LD is an indicator of arterial remodeling and thus can provide more information about the vascular health of a person.[48]

Narrowing of the carotid LD (stenosis) has been considered a major risk factor of ischemic stroke events.[49–51] We thus hypothesize the usage of carotid LD as a powerful EEGS model for CVD/stroke risk assessment.[52–54] An LD threshold of 6 mm was selected for risk-stratifying the patients into either high-risk or low-risk category.

3. Methods

3.1. Study cohort and image acquisition

A cohort of 202 Japanese patients (IRB approved) was recruited for this retrospective study from Toho University, Japan, and written consent was obtained from all participants. Left and right common carotid arteries of all the patients were examined using a B-mode ultrasound scanner (Aplio XG, Xario, Aplio XV, Toshiba Inc., Tokyo, Japan). In total, 395 CUS scans were collected by an expert sonographer (overall mean image resolution of 0.0529 mm per pixel). The protocol for CUS image acquisition was based on the consensus report of the American Society of Echocardiography[55] and has been discussed in detail in our previous studies.[56] All the CUS scans were retrospectively analyzed by two operators (an expert and a novice operator). The expert operator had 15 years of experience in ultrasonography and radiology. Compared with all the previously published studies with the same Japanese cohort,[17,39, 57–60] this study is unique in terms of a novel design for ML-based strategy for risk stratification by combining $CUSIP_{curr}$ and CRF (a class of AtheroEdge™ systems from AtheroPoint™, Roseville, CA, USA).[61]

3.2. Carotid ultrasound image phenotype measurements: feature set design

The feature set is comprised of 38 features: (a) 13 types of CRF and (b) 25 types of CUSIP.[17,32, 57, 58] The 13 types of CRF includes age, gender, hemoglobin A1c, fasting blood sugar, low-density lipoprotein, and high-density lipoprotein (HDL) cholesterol, total cholesterol (TC), a ratio of TC and HDL, hypertension, smoking, family history, triglyceride, and ultrasound-based carotid plaque score. The 25 types of CUSIP involved **(i)** five types of current CUSIP ($CUSIP_{curr}$) such as average cIMT (IMT_{ave}), maximal cIMT ($cIMT_{max}$), minimum cIMT ($cIMT_{min}$), variations in cIMT (IMTV), and total plaque area (TPA), **(ii)** five types of 10-year prediction of CUSIP ($CUSIP_{10yr}$) such as $cIMT_{ave10yr}$, $cIMT_{max10yr}$, $cIMT_{min10yr}$, $cIMTV_{10yr}$, and TPA_{10yr}, (iii) two types of AtheroEdge™ composite risk scores (AECRS) evaluated using $CUSIP_{curr}$ and $CUSIP_{10yr}$ such as $AECRS_{curr}$ and $AECRS_{10yr}$, (iv) 12 types of quadratic terms (harmonics) of these 12 image-based phenotypes (measured in (i), (ii), and (iii)), and finally, (v) an atherosclerotic plaque morphology-based feature called age-adjusted grayscale median (AAGSM) proposed by Kotsis et al.[32]

3.3. Machine learning-based risk stratification: conventional vs. integrated models

The supervised random forest (RF)-based ML algorithm (see Fig. 2) was used for CVD/stroke risk stratification.[38,39, 62] Data partitioning unit separates the input image database into training and testing datasets. The feature engineering block then extracts 38 types of training and testing features. The dotted rectangular box in Fig. 2 provides a choice to perform the CVD/stroke risk stratification either by CRF alone (conventional ML system) or by integrating CRF with CUSIP features (so-called integrated ML system[63]). The multivariate logistic regression (MLR) was then used for feature selection that resulted in 2 significant features (HT and TC) out of 13 CRF and 10 significant features (gender, age, HbA1c, TC, HT, Smoking, IMT_{min}, $AECRS_{10yr}$, $AECRS^2_{curr}$, and $AECRS^2_{10yr}$) out of 38 integrated features. These significant features were then used to train the ML-based RF classifier (for RF see Section C of Supplementary Material) under the supervision of training labels obtained from the EEGS. The trained ML coefficients were then

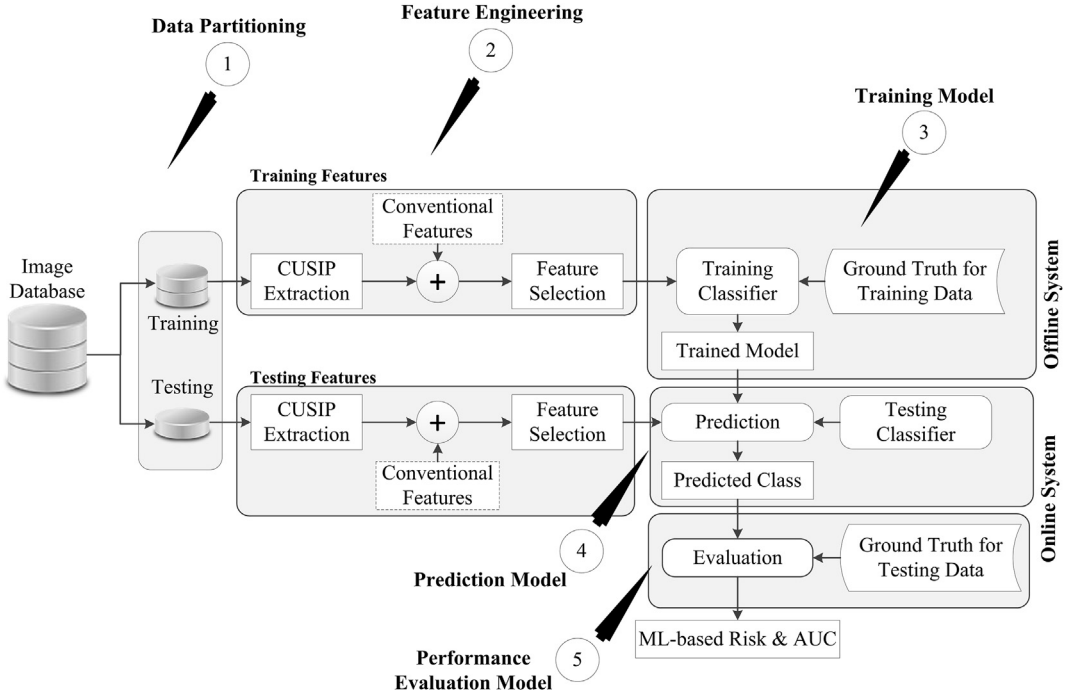

Fig. 2. The framework of the supervised machine learning system (Reproduced with permission from Authors and Springer publications[16]).

Table 1
Baseline characteristics of the patients divided into low-risk and high-risk classes.

C1	C2	C3	C4	C5	C6
SN	Parameters	Overall	High-Risk	Low-Risk	P-Val
R1	Total (n)	202	108	94	–
R2	Male, n (%)[a]	156 (77.23%)	79 (50.64%)	77 (49.36%)	0.003
R3	Age (years)[a]	68.97 ± 10.96	71.29 ± 9.07	66.30 ± 12.30	0.028
R4	HbA1c (%)	6.28 ± 1.11	6.34 ± 0.93	6.20 ± 1.29	0.615
R5	FBS (mg/dl)	121.21 ± 34.81	123.50 ± 36.42	118.59 ± 32.85	0.434
R6	LDL (mg/dl)	100.75 ± 31.48	100.38 ± 30.04	101.17 ± 33.22	0.270
R7	HDL (mg/dl)	50.49 ± 14.97	49.65 ± 14.66	51.45 ± 15.33	0.676
R8	TC (mg/dl)	174.33 ± 36.73	175.44 ± 35.14	173.05 ± 38.61	0.243
R9	TC/HDL	3.65 ± 1.01	3.74 ± 1.04	3.55 ± 0.97	0.500
R10	HT, n (%)[a]	147 (72.77%)	90 (61.22%)	57 (38.78%)	0.000
R11	SBP (mm Hg)[a]	134.55 ± 8.92	136.67 ± 7.49	132.13 ± 9.82	0.000
R12	DBP (mm Hg)[a]	87.28 ± 4.46	88.33 ± 3.74	86.06 ± 4.91	0.000
R13	Smoking, n (%)	81 (40.10%)	45 (55.56%)	36 (44.44%)	0.333
R14	FH, n (%)[a]	24 (11.88%)	17 (70.83%)	7 (29.17%)	0.000
R15	PS	9.09 (5.31)	10.19 (5.31)	7.84 (5.05)	0.523

HbA1c: Glycated Hemoglobin; LDL-C: Low-Density Lipoprotein Cholesterol; HDL-C: High-Density Lipoprotein Cholesterol; TC: Total Cholesterol; SBP: Systolic Blood Pressure; DBP: Diastolic Blood Pressure; FH: Family History; PS: Plaque Score.
[a] Significant Cofounding factors.

used to transform the features derived from the test data into the output risk classes (high-risk or low-risk). The performance of the ML system was evaluated using area-under-the-curve (AUC) against the gold standard test labels derived from EEGS.

3.4. Statistical analysis

SPSS23.0 and R Studio were used to perform statistical analysis. Independent sample *t*-test and chi-square tests were performed for the continuous and categorical variables, respectively. The baseline characteristics of the study population are presented as mean ± SD for continuous variables and numbers (percentages) for the categorical variables, respectively. Receiver operating characteristics analysis was performed to compare the AUC values of *AtheroRisk-integrated* against the *AtheroRisk-conventional* systems. Carotid LD with a threshold of 6 mm has been used as an EEGS to perform the performance evaluation using ROC analysis. The selection of LD threshold along with its sensitivity analysis is presented in Section B of the Supplementary Material. In order to test the validity of the recruited sample size, a power analysis was performed using a 95% confidence interval and a 5% error margin. This has resulted in an overall desired sample size of 334. The sample size used in this study (395 scans) was ~18% more than the required sample size of 334 for adequate power.

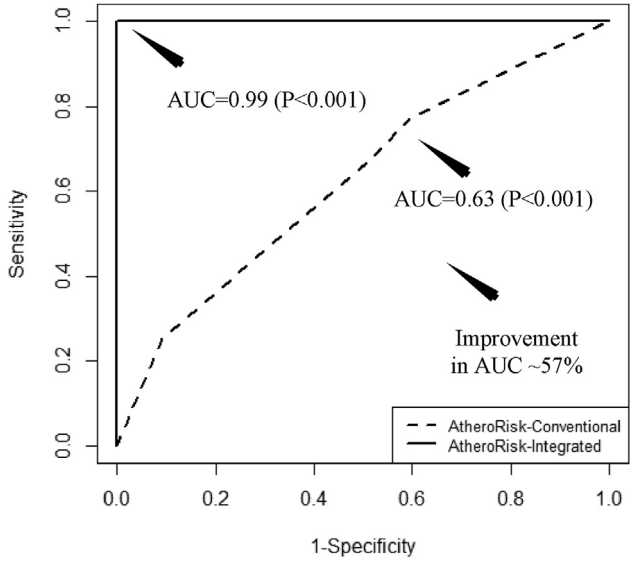

Fig. 3. Receiver operating characteristics and AUC values for *AtheroRisk-conventional* and *AtheroRisk-integrated* ML-based system using RF classifier.

4. Results

The baseline characteristics of the Japanese cohort are presented in Table 1. Out of 395 CUS scans, 317 (78.08%) images had a carotid plaque score greater than 5, and 131 (32.27%) images had $cIMT_{ave}$ ≥1.00 mm. The selected patients did not have any information about the atrial fibrillation with or without left atrial appendage clot, and therefore, it was not considered in the design of this study. From Table 1, it is clear that the baseline risk-profile of Japanese patients follow the high-risk category.

Using RF-based classifier, *AtheroRisk-integrated* showed the highest AUC (**AUC = 0.99**, P < 0.001) compared to *AtheroRisk-conventional* (**AUC = 0.63**, P < 0.001) for leave-one-out cross-validation protocol (see Fig. 3). These results demonstrated an overall improvement in the AUC of *AtheroRisk-integrated ML* system over *AtheroRisk-conventional* by **57.14**% with RF classifier. Due to the small sample size, we have used a leave-one-out cross-validation protocol. This has clearly indicated the potential role of the integrated set of features in *AtheroRisk-integrated* which consisted of both 13 CRF and 25 CUSIP (6 $CUSIP_{curr}$, 6 $CUSIP_{10yr}$, AAGSM, and 12 quadratic terms - harmonics), unlike *AtheroRisk-conventional* that used only 13 CRF.

In order to test the stability of the ML system, five current CUSIP were measured by two operators (an expert and a novice) at different time instants using AtheroEdge™ (AtheroPoint, Roseville, CA, USA)0.56, 64 Using these two different sets of CUSIP, the ML-based system was trained and tested against EEGS. The mean risk stratification accuracy and AUC for two sets of measurements were differed by less than 5% (Accuracy: 93.15% *vs.* 96.22% and AUC 0.92 *vs.* 0.96, p < 0.001). The precision-of-merit and figure-of-merit was **96**% with an overall mean absolute error of less than ±5%. This indicated CUSIP used for risk stratification was highly stable and reliable.

5. Discussion

This study validated our hypothesis that shows a greater risk predictive ability for ML-based systems using integrated risk factors

Table 2
Machine learning-based CVD/Stroke risk stratification.

#SN	C1	C2	C3	C4	C5	C6	C7	C8	C9	C10	C11
	Authors	AT (Modality)	Features Types	TF	Classifier Type	Ground Truth	N*	TI	Training Protocol	Performance Evaluation	Benchmarking
R1	Kariacou et al[17] (2012)	Carotid (CUS)	Image-based Texture	27	SVM, LR	Follow-up data labels	108	–	–	ACC (77%)	–
R2	Acharya et al[18] (2013)	Carotid (CUS)	Grayscale Features	17	SVM, GMM, RBPNN, DT, kNN, NBC, FC	Labels from Physicians	445	492	K3	DB1:Accuracy (93.1%) DB1:Accuracy (85.3%)	–
R3	Acharya et al[72] (2014)	Carotid (CUS)	Phenotypes & HoS Features	7	SVM, RBPNN, kNN, DT	Labels from physicians	59	118	K10	Accuracy (99.1%)	–
R4	Gastounioti et al[19] (2015)	Carotid (CUS)	Kinematics Features	1236	SVM	Follow-up data labels	56	4200	–	Accuracy (88%)	Against kNN, PNN, DT, DA
R5	Araki et al[20] (2017)	Carotid (CUS)	Image-based Texture Features	16	SVM	LD-based risk labels	204	407	K5, K10, JK	Accuracy (NW: 95.08% & FW: 93.47%)	–
R6	Saba et al[21] (2017)	Carotid (CUS)	Image-based Texture	16	SVM	LD-based risk labels	204	407	K10	Accuracy (NW: 98.83% & FW: 98.55%)	–
R7	Weng et al[22] (2017)	–	CRF	30	RF, LR, GBM, ANN	Follow-up data labels	378256	–	K4	AUC: 0.764	Against PCRS
R8	Kakadiaris et al[23] (2018)	–	CRF	9	SVM	Follow-up data labels	6459	–	K2	Se (86%), Sp (95%), AUC (0.92)	Against PCRS
R9	Proposed (2019)	Carotid (CUS)	Integrated Features	38	RF	Labels from physicians	202	395	K2, K5, K10, JK	AUC: **0.99**	Against Conventional

CUS: Carotid ultrasound, LR: Logistic Regression, SVM: Support Vector Machine; Se: Sensitivity, Sp: Specificity; DWT: Discrete Wavelet Transform, kNN: K-Nearest Neighbor, RBPNN: Radial Basis Probabilistic Neural Network, GMM: Gaussian Mixture Model, NBC: Naïve Bays Classifier, FC: Fuzzy Classifier, DB: Database, HoS: Higher order Spectra, LBP: Local Binary Pattern, FDR: Fisher Discriminant Ratio, WRS: Wilcoxon Rank-Sum, PCA: Principal Component Analysis, DA: Discriminant Analysis, MLP: Multilayer Perceptron, RF: Random Forest, BS: Brier Score, QNN: Quantum Neural Network, IGR: Information Gain Ranking, MDMST: Minimal Depth of Maximal Subtree, SOM: Self Organization Map, FRS: Framingham Risk score, PCRD: Pooled Cohort Risk Score.

(**AUC = 0.99**, P < 0.001) compared to the CRF alone (**AUC = 0.63**, P < 0.001).

5.1. Benchmarking

Table 2 chronologically compared the proposed *AtheroRisk-integrated* system against the eight ML-based studies (row R1 to R8) using eleven attributes (column C1 to C11). Nearly all the previous studies used either the conventional blood biomarkers and clinical parameters, or the grayscale image-based features for CVD risk assessment. The conventional risk factors do not capture the morphological variations in the blood vessels, which, however, can be possible using the image-based phenotypes.16–18, 32, 36, 38, 65 Thus, integrating this CUSIP with CRF can provide a stronger assessment of risk assessment.18, 65, 66 Our study (row R9) is the only study that combined the CRF with the CUSIP leading to 38 features. As a result, the integrated RF-based ML system demonstrated an AUC~**0.99**, which is far better than the studies that used CRF or image-based grayscale features alone.

5.2. Effect of using cIMT as EEGS for CVD/stroke risk assessment

Pignoli et al67 presented the use of B-mode ultrasound for visualizing the cIMT. Since then, the use of cIMT as a preventive tool for the CVD/stroke risk assessment is continuously debated.5, 55, 68–73 cIMT has been also been tested as a surrogate marker of CVD/stroke events in the literature.74–82 Thus, we investigated its effect as EEGS for ML-based CVD/stroke risk stratification. With cIMT as EEGS, *AtheroRisk-integrated* showed a superior performance (AUC = **0.95,** P < 0.001) compared to the *AtheroRisk-conventional* (AUC = **0.59,** P < 0.001) with an overall improvement in AUC of ~61%. It should be noted, cIMT as EEGS reported the highest improvement in AUC value (~61%) compared to LD as EEGS (~57%). However, it is also important to note that in our current study using cIMT as EEGS may lead to a bias effect. This is because the feature set of 38 risk factors was derived by using 16 types of cIMT values (four current cIMT, four 10-year cIMT, and eight harmonics (quadratics terms) of cIMT). Thus, carotid LD was considered to be the best choice for EEGS.

5.3. A note on the therapeutic implications of ML-based risk stratification

The primary objective of the risk stratification system is to predict the risk profile of the patients and stratify them into one of the several CVD/stroke risk categories such as low-risk, moderate-risk, or high-risk. In general practice, risk assessment systems aid physicians in deciding the need and strength of the medications such as lipid-lowering medications (for example pravastatin, atorvastatin, and simvastatin)83 or diabetes control medication (for example metformin)0.84 Compared with traditional risk prediction models, ML-based risk assessment systems have the promise to be more accurate37 and avoid the under or overestimation of CVD/stroke risk.

5.4. Strength, limitations, future scope

Although the study results support our hypothesis, we believe that additional investigations may allow for more progress in ML-based strategies for risk stratification. Even though the pilot study had a small cohort size with acceptable power analysis for sample size test, the ML had an ability to adjust the variations of the image phenotypes when combined with the CRF during training to compute the predicted risk on test patients. Note that the ML system did use the surrogate image-based biomarker (lumen diameter) as EEGS, 17, 19, 32, 39, 58–60, 85 which may add to a slight bias in the overall estimation of predicted risk. Thus, we need a larger multi-ethnic, multi-center cohort for stronger validation and performance evaluation of ML systems using primary endpoints. At last, the current study did not consider the effect of carotid stenosis, which is a well-established atherosclerosis-driven CVD/stroke biomarker,[20–23] and hence, needs further validation. The proposed ML-based integrated system can be extended by incorporating inflammatory markers, renal disease markers, grayscale features that

are also associated with the risk of CVD and stroke, and further be converted as an online platform for risk stratification.[24] Even though our LD estimation methods were scale-space based, the system can be extended using deep learning-based models for LD estimation.[25–27] Similarly, image phenotypes can also be computed using deep learning-based solutions.[28]

6. Conclusion

We presented a novel ML system that integrated 25 carotid ultrasound image-based phenotypes (CUSIP) with 13 conventional risk factors (CRF) factors. We proved our hypothesis that *AtheroRisk-integrated* is far superior to *AtheroRisk-conventional* for using Random Forest classifier. Our results demonstrated that *AtheroRisk-integrated* showed an overall improvement of **57.14**% in the AUC when using an RF-based classifier. Since our machine learning systems were generalized, it can, therefore, be extended to deep learning-based paradigms.

What is already known?

Generally, statistically derived and machine learning-based risk prediction models use either conventional clinical parameters for CVD risk assessment.

What this study adds:

Integration of conventional clinical risk factors with carotid ultrasound image phenotypes can offer higher risk stratification ability.

Conflicts of interest

All authors have none to declare.

Financial Support/grants

None.

Acknowledgements

None.

Appendix A. Supplementary data

Supplementary data to this article can be found online at https://doi.org/10.1016/j.ihj.2020.06.004.

References

1. World Health Organization. Cardiovascular disease Available at: http://www.who.int/mediacentre/factsheets/fs317/en/
2. Pearson TA, Blair SN, Daniels SR, et al. AHA guidelines for primary prevention of cardiovascular disease and stroke: 2002 update: consensus panel guide to comprehensive risk reduction for adult patients without coronary or other atherosclerotic vascular diseases. *Circulation*. 2002;106:388–391.
3. *Lipid Modification: Cardiovascular Risk Assessment and the Modification of Blood Lipids for the Primary and Secondary Prevention of Cardiovascular Disease*. London: Royal College of General Practitioners.; 2008.
4. Organization WH. *Package of Essential Noncommunicable (PEN) Disease Interventions for Primary Health Care in Low-Resource Settings*. 2010.
5. Goff DC, Lloyd-Jones DM, Bennett G, et al. 2013 ACC/AHA guideline on the assessment of cardiovascular risk: a report of the American college of cardiology/American heart association task force on practice guidelines. *J Am Coll Cardiol*. 2014;63:2935–2959.
6. Lalor E, Boyden A, Cadilhac D, et al. *Guidelines for the Management of Absolute Cardiovascular Disease Risk*. 2012.
7. Reiner Z, Catapano AL, De Backer G, et al. ESC/EAS Guidelines for the management of dyslipidaemias: the Task Force for the management of dyslipidaemias of the European Society of Cardiology (ESC) and the European Atherosclerosis Society (EAS). *Eur Heart J*. 2011;32:1769–1818.
8. Reiner Ž, Catapano AL, De Backer G, et al. ESC/EAS guidelines for the management of dyslipidaemias: the task force for the management of dyslipidaemias of the European society of cardiology (ESC) and the European atherosclerosis society (EAS). *Eur Heart J*. 2011;32:1769–1818.
9. van Staa T-P, Gulliford M, Ng ES-W, Goldacre B, Smeeth L. Prediction of cardiovascular risk using Framingham, ASSIGN and QRISK2: how well do they predict individual rather than population risk? *PloS One*. 2014;9, e106455.
10. Allan GM, Garrison S, McCormack J. Comparison of cardiovascular disease risk calculators. *Curr Opin Lipidol*. 2014;25:254–265.
11. Coleman RL, Stevens RJ, Retnakaran R, Holman RR. Framingham, SCORE, and DECODE risk equations do not provide reliable cardiovascular risk estimates in type 2 diabetes. *Diabetes Care*. 2007;30:1292.
12. Chien K-L, Lin H-J, Su T-C, Chen Y-Y, Chen P-C. Comparing the consistency and performance of various coronary heart disease prediction models for primary prevention using a national representative cohort in Taiwan. *Circ J*. 2018;82(7):1805–1812. CJ-17-0910.
13. Bansal D, Nayakallu RS, Gudala K, Vyamasuni R, Bhansali A. Agreement between Framingham risk score and United Kingdom Prospective Diabetes Study risk engine in identifying high coronary heart disease risk in North Indian population. *Diabetes Metabol J*. 2015;39:321–327.
14. Alemao E, Cawston H, Bourhis F, et al. Comparison of cardiovascular risk algorithms in patients with vs without rheumatoid arthritis and the role of C-reactive protein in predicting cardiovascular outcomes in rheumatoid arthritis. *Rheumatology*. 2017;56:777–786.
15. Crowson CS, Rollefstad S, Kitas GD, Van Riel PL, Gabriel SE, Semb AG. Challenges of developing a cardiovascular risk calculator for patients with rheumatoid arthritis. *PloS One*. 2017;12, e0174656.
16. Jamthikar A, Gupta D, Khanna NN, et al. A special report on changing Trends in preventive stroke/cardiovascular risk assessment via B-mode ultrasonography. *Curr Atherosclerosis Rep*. 2019;21:25.
17. Khanna NN, Jamthikar AD, Gupta D, et al. Effect of carotid image-based phenotypes on cardiovascular risk calculator: AECRS1. 0. *Med Biol Eng Comput*. 2019;57:1553–1566.
18. Khanna NN, Jamthikar AD, Gupta D, et al. Performance evaluation of 10-year ultrasound image-based stroke/cardiovascular (CV) risk calculator by comparing against ten conventional CV risk calculators: a diabetic study. *Comput Biol Med*. 2019;105:125–143.
19. Viswanathan V, Jamthikar AD, Gupta D, et al. Integration of eGFR biomarker in image-based CV/Stroke risk calculator: a south Asian-Indian diabetes cohort with moderate chronic kidney disease. *Int Angiol*. 2020. https://doi.org/10.23736/S0392-9590.20.04338-2. In press.
20. Viswanathan V, Jamthikar AD, Gupta D, et al. Low-cost preventive screening using carotid ultrasound in patients with diabetes. *Front Biosci (Landmark Ed)*. 2020;25:1132–1171.
21. Molinari F, Pattichis CS, Zeng G, et al. Completely automated multiresolution edge snapper—a new technique for an accurate carotid ultrasound IMT measurement: clinical validation and benchmarking on a multi-institutional database. *IEEE Trans Image Process*. 2012;21:1211–1222.
22. Suri JS, Kathuria C, Molinari F. *Atherosclerosis Disease Management*. Springer Science & Business Media; 2010.
23. Viswanathan V, Jamthikar A, Gupta D, et al. Low-cost preventive screening using carotid ultrasound in patients with diabetes. *Front Biosci (Landmark Ed)*. 2020;25:1132.
24. Radeva P, Suri JS. Vascular and intravascular imaging Trends, analysis, and challenges. In: Radeva Petia, Suri Jasjit S, eds. *Plaque Characterization. Vascular and Intravascular Imaging Trends, Analysis, and Challenges, Volume 2; Plaque characterization*. Bristol, UK: IOP Publishing; 2019:; vol. 2.
25. Khanna NN, Jamthikar AD, Gupta D, et al. Rheumatoid arthritis: atherosclerosis imaging and cardiovascular risk assessment using machine and deep learning–based tissue characterization. *Curr Atherosclerosis Rep*. 2019;21:7.
26. Amato M, Montorsi P, Ravani A, et al. Carotid intima-media thickness by B-mode ultrasound as surrogate of coronary atherosclerosis: correlation with quantitative coronary angiography and coronary intravascular ultrasound findings. *Eur Heart J*. 2007;28:2094–2101.
27. Bots ML. Carotid intima-media thickness as a surrogate marker for cardiovascular disease in intervention studies. *Curr Med Res Opin*. 2006;22:2181–2190.
28. Molinari F, Meiburger KM, Saba L, et al. *Automated Carotid IMT Measurement and its Validation in Low Contrast Ultrasound Database of 885 Patient Indian Population Epidemiological Study: Results of AtheroEdge® Software. Multi-Modality Atherosclerosis Imaging and Diagnosis*. Springer; 2014:209–219.
29. Molinari F, Zeng G, Suri JS. Intima-media thickness: setting a standard for a completely automated method of ultrasound measurement. *IEEE Trans Ultrason Ferroelectrics Freq Contr*. 2010;57:1112–1124.
30. Saba L, Meiburger KM, Molinari F, et al. Carotid IMT variability (IMTV) and its validation in symptomatic versus asymptomatic Italian population: can this be a useful index for studying symptomaticity? *Echocardiography*. 2012;29:1111–1119.

31. Saba L, Montisci R, Molinari F, et al. Comparison between manual and automated analysis for the quantification of carotid wall by using sonography. A validation study with CT. *Eur J Radiol*. 2012;81:911–918.
32. Kotsis V, Jamthikar AD, Araki T, et al. Echolucency-based phenotype in carotid atherosclerosis disease for risk stratification of diabetes patients. *Diabetes Res Clin Pract*. 2018;143:322–331.
33. Acharya UR, Sree SV, Krishnan MMR, et al. Atherosclerotic risk stratification strategy for carotid arteries using texture-based features. *Ultrasound Med Biol*. 2012;38:899–915.
34. Acharya UR, Sree SV, Ribeiro R, et al. Data mining framework for fatty liver disease classification in ultrasound: a hybrid feature extraction paradigm. *Med Phys*. 2012;39:4255–4264.
35. Acharya U, Sree SV, Mookiah M, et al. Computed tomography carotid wall plaque characterization using a combination of discrete wavelet transform and texture features: a pilot study. *Proc IME H J Eng Med*. 2013;227:643–654.
36. Boi A, Jamthikar AD, Saba L, et al. A survey on coronary atherosclerotic plaque tissue characterization in intravascular optical coherence tomography. *Curr Atherosclerosis Rep*. 2018;20:33.
37. Kakadiaris IA, Vrigkas M, Yen AA, Kuznetsova T, Budoff M, Naghavi M. Machine learning outperforms ACC/AHA CVD risk calculator in MESA. *J Am Heart Assoc*. 2018;7, e009476.
38. Jamthikar A, Gupta D, Khanna NN, et al. A low-cost machine learning-based cardiovascular/stroke risk assessment system: integration of conventional factors with image phenotypes. *Cardiovasc Diagn Ther*. 2019;9:420–430.
39. Jamthikar A, Gupta D, Saba L, et al. Cardiovascular/stroke risk predictive calculators: a comparison between statistical and machine learning models. *Cardiovasc Diagn Ther*; 2020. In press http://cdt.amegroups.com/article/view/37250.
40. Weng SF, Reps J, Kai J, Garibaldi JM, Qureshi N. Can machine-learning improve cardiovascular risk prediction using routine clinical data? *PloS One*. 2017;12, e0174944. Note: All the references beyond 41 are provided as part of Section D of the Supplementary Material.